

Transition control of the Blasius boundary layer using passivity

Christopher J. Damaren

Aerospace Systems

ISSN 2523-3947

AS

DOI 10.1007/s42401-018-0021-0



Your article is protected by copyright and all rights are held exclusively by Shanghai Jiao Tong University. This e-offprint is for personal use only and shall not be self-archived in electronic repositories. If you wish to self-archive your article, please use the accepted manuscript version for posting on your own website. You may further deposit the accepted manuscript version in any repository, provided it is only made publicly available 12 months after official publication or later and provided acknowledgement is given to the original source of publication and a link is inserted to the published article on Springer's website. The link must be accompanied by the following text: "The final publication is available at link.springer.com".



Transition control of the Blasius boundary layer using passivity

Christopher J. Damaren¹

Received: 19 July 2018 / Revised: 29 October 2018 / Accepted: 4 December 2018
© Shanghai Jiao Tong University 2018

Abstract

The control problem for linearised three-dimensional perturbations about a nominal laminar boundary layer over a flat plate (the Blasius profile) is considered. With a view to preventing the laminar to turbulent transition, appropriate inputs, outputs, and feedback controllers are synthesised that can be used to stabilise the system. The linearised Navier–Stokes equations are reduced to the Orr–Sommerfeld and Squire equations with wall-normal velocity actuation entering through the boundary conditions on the wall. An analysis of the work-energy balance is used to identify an appropriate sensor output that leads to a passive system for certain values of the streamwise and spanwise wavenumbers. Even when the system is unstable, it is demonstrated that strictly positive real feedback can stabilise this system using the special output.

Keywords Transition Control · Boundary Layer · Passivity

1 Introduction

The viscous effects in unseparated flow over a body are concentrated in a thin layer adjacent to the body's surface known as the boundary layer. The no-slip condition for the fluid velocity on this surface leads to a form of drag known as skin friction drag. The size of this force depends strongly on whether the flow is laminar or turbulent with laminar boundary layers producing less drag. Hence, there is a great deal of motivation to prevent transition between the two flow regimes from occurring.

Historically, the transition problem has been studied by linearising the Navier–Stokes equations about a nominal velocity profile consisting of a baseline laminar flow and addressing the stability of small perturbations [10,17]. For boundary layer flows over a flat plate, this profile has typically been taken to be the two-dimensional Blasius solution [16]. If a two-dimensional spatial Fourier transform is taken of the linearised equations (corresponding to assuming spatially oscillating perturbations in the streamwise and spanwise directions), one arrives at the Orr–Sommerfeld equation describing the wall-normal velocity component and

the Squire equation describing the wall-normal vorticity component. Transition can be studied by determining the eigenvalues of the Orr–Sommerfeld/Squire model governing the perturbations (Drazin and Reid 2001).

It has been noted by experimentalists that transition typically occurs at Reynolds numbers (based on distance along the plate) that are smaller than those predicted by linear eigenvalue theory [10]. It has been postulated that large transient growth in the flow perturbations can trigger transition via nonlinear mechanisms before the linear instability mechanism occurs. Transient growth in the Blasius boundary layer was studied by Butler and Farrell [7], who noted that at some Reynolds numbers, the worst case transient growth occurred at streamwise wavenumbers that were zero and nonzero spanwise wavenumbers.

Linear theory can be exploited using the associated models to develop feedback controllers which address stabilisation at those Reynolds numbers and wavenumbers where the instabilities would otherwise occur. Active feedback control requires the introduction of appropriate sensors and actuators and the design of feedback controllers. The history and use of linear state-space models based on the Orr–Sommerfeld/Squire system to design feedback controllers is described by Bewley [4].

Active control design has been investigated for several flows with emphasis on plane Poiseuille flow [5,12] and the Blasius boundary layer [1,2]. The Poiseuille flow corresponds to the fully developed flow in a channel between

Professor and Director, University of Toronto Institute for Aerospace Studies, 4925 Dufferin Street. Associate Fellow AIAA.

✉ Christopher J. Damaren
damaren@utias.utoronto.ca

¹ University of Toronto, Toronto, ON M3H 5T6, Canada

two parallel infinite plates and the Blasius boundary layer is the two-dimensional laminar flow over a semi-infinite flat plate. This paper will concentrate on the latter case. The use of linear models to develop linear controllers for what is generally considered to be a nonlinear phenomenon (transition to turbulence) has been championed by many authors who have argued that linear control systems based on linear models can deal with the initial linear amplification of disturbances, thus preventing the subsequent nonlinear transition behaviour [13].

The type and location of the sensors and actuators has a profound effect on the achievable stability, performance, and robustness of a feedback strategy. Sensor and actuator locations have been considered by Belson et al. [2] in the Blasius case. A very useful paradigm for robust feedback controller design is passivity-based control. Passive systems [9] are those that only store or dissipate energy. Strict passivity is a stronger property than passivity and corresponds to systems that only consume (dissipate) energy. The passivity theorem [9] states that the negative feedback interconnection of a passive system and a strictly passive system (with finite gain) is L_2 -stable, that is, L_2 (finite energy) inputs produce L_2 (finite energy) outputs.

In a previous work [8], we studied the passivity property in two dimensions in the context of the Orr–Sommerfeld equation with actuation inputs implemented as wall-normal velocity. A dual output (based on energy analysis) was shown to be the second spatial derivative (normal direction) of the streamwise velocity perturbation at the wall. Although passivity of the model relating this input and output could not be demonstrated, it was shown that an appropriate closed-loop system could be made passive with a baseline Poiseuille flow but not with a Blasius flow. Passivity ideas have been employed by Sharma et al. [18] and Heins et al. [11] in the stabilisation of a Poiseuille flow (the fully developed flow in a channel between two parallel plates).

The paper is organised as follows. Section 2 defines the key notions involving passivity. In Sect. 3, we resume the passivity analysis from [8], this time in three spatial dimensions using both the Orr–Sommerfeld and Squire equations. In Sect. 4, spatial discretisation of the Orr–Sommerfeld and Squire equations is accomplished using Hermite cubic finite elements to describe the wall-normal velocity and vorticity components. This approach was originally used for the Orr–Sommerfeld equation with Poiseuille flows by Mamou and Khalid [14]. In Sect. 5, stabilisation using the passivity-based output is demonstrated at a Reynolds number and wavenumber pair that is open-loop unstable. Section 6 presents some concluding remarks.

2 Feedback controller design

2.1 Passivity and feedback design

Consider the feedback system shown in Fig. 1 where $d_1(t)$, $d_2(t)$, $m_1(t)$, and $m_2(t)$ are functions of time t . Generically, $m \in L_2$ if the L_2 -norm satisfies $\|m\|_2 \triangleq \sqrt{\int_0^\infty m^T(t)m(t) dt} < \infty$ (the symbol $(\)^T$ denotes the matrix transpose and $(\)^H$ denotes the complex-conjugate transpose). We also have, $m \in L_{2e}$ (the extended L_2 -space) if $\|m\|_{2T} \triangleq \sqrt{\int_0^T m^T(t)m(t) dt} < \infty, 0 \leq T < \infty$. Note that $L_2 \subset L_{2e}$. Consider a system $m(t) = (\mathcal{G}e)(t)$ where the operator $\mathcal{G} : L_{2e} \rightarrow L_{2e}$ (possibly nonlinear and time-varying) maps the input $e \in L_{2e}$ into the output $m \in L_{2e}$. The gain of \mathcal{G} (which is the induced norm on L_2) is defined to be $\|\mathcal{G}\| = \sup_{0 \neq e \in L_2} \|\mathcal{G}e\|_2 / \|e\|_2$.

If the system \mathcal{G} is square (the number of inputs in e is equal to the number of outputs in m), the operator \mathcal{G} is defined to be strictly passive if $\int_0^T m^T(t)e(t) dt = \int_0^T e^T(t)\mathcal{G}e(t) dt \geq \delta + \epsilon \int_0^T e^T(t)e(t) dt, \forall e \in L_{2e}, 0 \leq T < \infty$, for some $\epsilon > 0$ and real constant δ which may depend on the initial conditions of \mathcal{G} . If $\epsilon = 0$, the system is passive.

If \mathcal{G} is linear time-invariant (LTI) (and finite dimensional), it is describable by the standard state-space model

$$\dot{x}(t) = Ax(t) + Be(t) \tag{1}$$

$$m(t) = Cx(t) + De(t) \tag{2}$$

where $(\dot{\ })$ denotes the time derivative. This system can be described using transfer functions: $m(s) = G(s)e(s)$ where $m(s)$ denotes the Laplace transform of $m(t)$ (a common abuse of notation) and $G(s)$ is the system transfer (function) matrix. The quantity s denotes the complex-valued Laplace transform variable and $i = \sqrt{-1}$. Note that $G(s) = C(sI - A)^{-1}B + D$ is the transfer matrix corresponding to the state-space model in Eqs. (1) and (2). Here, I is the identity matrix of appropriate dimension. If the system is minimal, i.e., it is controllable and observable, then L_2 -stability of \mathcal{G} ($e \in L_2$ implies that $m = \mathcal{G}e \in L_2$) corresponds to the matrix A having eigenvalues with negative real parts. For stable LTI systems, the gain can be shown (Vidyasagar, 1992) to be $\|\mathcal{G}\| = \|G(s)\|_\infty = \sup_{\omega \in \mathcal{R}} \bar{\sigma}[G(i\omega)]$ where $\bar{\sigma}$ denote the largest singular value.

Passive LTI systems of this form correspond to the case where $G(s)$ is a positive real (PR) transfer function. When $G(s)$ is a proper real rational matrix function of s , it is positive real if no element of $G(s)$ has a pole in $\Re\{s\} > 0$; $\text{He}[G(i\omega)] = (1/2)[G(i\omega) + G^H(i\omega)] \geq 0$ for all real ω with $i\omega$ not a pole of $G(s)$ ($\text{He}(\)$ denotes the Hermitian part of a square matrix); and if $i\omega_0$ is a pole of any element

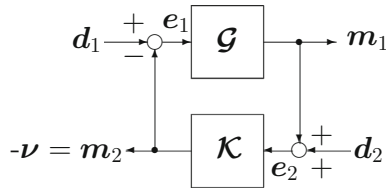


Fig. 1 Feedback system

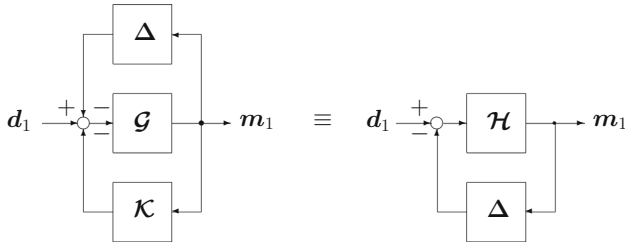


Fig. 2 Closed-loop system with perturbation

of $G(s)$, it is at most a simple pole and the residue matrix $\lim_{s \rightarrow i\omega_0} (s - i\omega_0)G(s)$ is non-negative definite Hermitian.

A stronger property than positive real is strictly positive real (SPR). A proper real rational matrix function of s , $K(s)$, is SPR if no element of $K(s)$ has a pole in $\Re\{s\} \geq 0$; $\text{He}[K(i\omega)] > \mathbf{0}$ for all real $\omega \in (-\infty, \infty)$; and $\lim_{\omega \rightarrow \infty} \omega^2 \text{He}[K(i\omega)] > \mathbf{0}$. A system with transfer matrix $K(s) + \epsilon I$ is strictly passive with finite gain if $K(s)$ is SPR and $\epsilon > 0$. The importance of passivity for feedback design lies in the passivity theorem [9], which addresses the feedback system shown in Fig. 1. One form of the passivity theorem states that if G is passive and K is strictly passive with finite gain, then $d_1, d_2 \in L_2$ implies that $e_1, e_2, m_1, m_2 \in L_2$.

Another useful property of passive systems stems from the fact that negative feedback interconnections of passive systems are also passive. Also, the negative feedback interconnection of a passive system and a strictly passive one is also strictly passive. This has important repercussions for systems with uncertainty modelled as a passive system in negative feedback with a nominal plant (see Fig. 2 where the uncertainty is modelled as an operator $\Delta : L_{2e} \rightarrow L_{2e}$). It has been noted by Sharma et al. [18] that the nonlinearities in the Navier–Stokes equations can be modelled as passive uncertainty in negative feedback with a linearised model. With reference to Fig. 2, if the negative feedback interconnection of G and K is strictly passive (this system is denoted by \mathcal{H}) and the perturbation Δ is passive, then the closed-loop system is L_2 -stable, i.e., $d_1 \in L_2$ implies that $m_1 \in L_2$.

It should be noted that although passivity of G and strict passivity of K are sufficient for \mathcal{H} to be strictly passive, they are not necessary conditions. An interesting design problem for LTI systems is the following: given $G(s)$ (not necessarily passive), find $K(s)$ to render $H(s) = G(s)[I + K(s)G(s)]^{-1}$

SPR [15] which would mean that the system in Fig. 2 is L_2 -stable for passive Δ .

When the system \mathcal{H} in Fig. 2 is not passive, some robustness properties can still be obtained using the notions of conic sectors and the conic sector theorem. Following Zames [20] and Bridgeman and Forbes [6], the system $\mathcal{H} : L_{2e} \rightarrow L_{2e}$ is in the conic sector $[a_c, b_c]$ (denoted $\mathcal{H} \in \text{cone}[a_c, b_c]$) where $a_c < b_c$ and $b_c > 0$ if

$$-\frac{1}{b_c} \|\mathcal{H}e\|_{2T}^2 + \left(1 + \frac{a_c}{b_c}\right) \int_0^T e^T(t) \mathcal{H}e(t) dt - a_c \|e\|_{2T}^2 \geq 0, \quad (3)$$

$\forall e \in L_{2e}, T \geq 0$. It is strictly in the conic sector (denoted $\mathcal{H} \in \text{cone}(a_c, b_c)$) if $\mathcal{H} \in \text{cone}[a_c + \epsilon, b_c - \epsilon]$ for some small $\epsilon > 0$. From this definition, it clear that for a passive system $\mathcal{H} \in \text{cone}[0, \infty]$.

We will be interested in systems $\mathcal{H} \in \text{cone}[a_c, \infty]$ with $a_c < 0$. For a stable LTI system with transfer matrix $H(s)$, a simple (temporal) Fourier transform of Eq. (3) shows that

$$\text{He}[H(i\omega)] \geq a_c I, \quad \forall \omega \in \mathcal{R} \quad (4)$$

The conic sector theorem [20] as presented by Bridgeman and Forbes [6] states that the system in Fig. 2 is L_2 -stable if $\mathcal{H} \in \text{cone}[a_c, b_c]$ with $a_c < 0$ and $\Delta \in \text{cone}(-1/b_c, -1/a_c)$. In particular, we have L_2 stability if $\mathcal{H} \in \text{cone}[a_c, \infty]$ with $a_c < 0$ and $\Delta \in \text{cone}(0, -1/a_c)$. This implies that Δ is passive and it is possible to show that $\|\Delta\| < -1/a_c$. Hence, a stable LTI system \mathcal{H} with transfer matrix satisfying Eq. (4) in negative feedback with a passive system Δ whose L_2 gain is less than $-1/a_c$ will be L_2 -stable.

2.2 Strictly positive real design

Consider the case where G and K correspond to LTI systems with transfer matrices $G(s) = C(sI - A)^{-1}B + D$ and $K(s) = K_c(sI - A_c)^{-1}K_e$. Consider the plant model $\dot{x} = Ax + Bv$ (i.e., $d_1 = d_2 = 0$). A state feedback gain can be chosen to minimise the quadratic performance index

$$J_{\text{LQR}} = \frac{1}{2} \int_0^\infty (x^T(t) Q x(t) + v^T(t) R v(t)) dt \quad (5)$$

where the weighting matrices are chosen such that Q is symmetric and non-negative definite and R is selected to be symmetric and positive definite. This is the well-known linear quadratic regulator (LQR) which has the feedback solution $v(t) = -K_{\text{LQR}}x(t)$ with feedback gain $K_{\text{LQR}} = R^{-1}B^T P_{\text{LQR}}$. The matrix P_{LQR} is the solution of the algebraic Riccati equation $P_{\text{LQR}}A + A^T P_{\text{LQR}} - P_{\text{LQR}}BR^{-1}B^T P_{\text{LQR}} + Q = 0$.

Our approach to SPR design is based on [3]. The SPR controller is given by $K_c = K_{LQR}$, $A_c = A - BK_{LQR}$, and $K_e = P^{-1}K_c^T$ where

$$PA_c + A_c^T P = -Q \tag{6}$$

The non-negative definite matrix Q and the positive definite matrices R (used to design K_{LQR}) and Q_c are free design parameters. Eq. (6) coupled with $PK_e = K_c^T$ ensures that the control system satisfies the Kalman–Yakubovich Lemma [19] and hence is SPR.

2.3 Model order reduction

The controller designs presented above have assumed a full-order model. A controller with a reduced number of states can be developed by employing a controller design using a reduced-order model. Assume that the system $G(s)$ has been transformed to modal form. Assuming that the eigenvalues of A , λ_i , are distinct, the modal system is given by

$$G(s) = \left[\begin{array}{cccc|c} \lambda_1 & 0 & \cdots & 0 & \hat{b}_1^H \\ 0 & \lambda_2 & \cdots & 0 & \hat{b}_2^H \\ \vdots & \vdots & \ddots & \vdots & \vdots \\ 0 & 0 & \cdots & \lambda_n & \hat{b}_n^H \\ \hline \hat{c}_1 & \hat{c}_2 & \cdots & \hat{c}_n & D \end{array} \right] \tag{7}$$

If distinct eigenvalues are assumed, the conditions for modal controllability and modal observability are $\|\hat{b}_\alpha\| > 0$ and $\|\hat{c}_\alpha\| > 0$. A reduced-order model can be created using those modes with the largest values of $\|\hat{b}_\alpha\| \cdot \|\hat{c}_\alpha\|$. Hence, they are the most controllable/observable as measured by the product of the modal controllability and observability norms.

2.4 Motivation for a passivity analysis and passivity-based control

This paper seeks to analyse the passivity properties of the linearised system relating the wall-normal velocity as actuation to an appropriate sensor output in the case of the flow perturbations acting on the Blasius boundary layer. Hence, the passivity analysis answers the question “what should be measured if the actuation is wall-normal blowing and suction?” Determining an output that leads to a passive system produces a system that is easy to stabilise since any strictly passive negative feedback controller leads to this result. Hence, a large family of stabilising controllers is available. Using a strictly passive feedback controller (or an SPR controller in the LTI case), one produces a closed-loop system whose stability is robust with respect to passive perturbations connected in a feedforward arrangement (which continues to produce a passive plant)

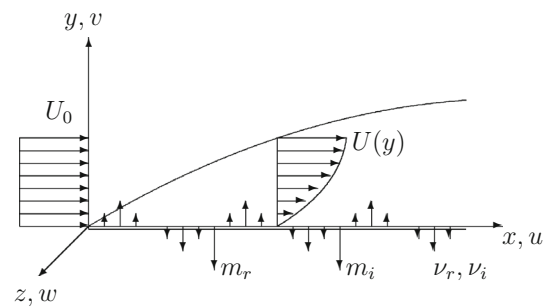


Fig. 3 Blasius boundary layer

or a negative feedback arrangement (which is stable if the nominal closed-loop system is strictly passive). As will be examined in a later section, the feedforward perturbation could correspond to the system nonlinearities. The feedback perturbation could correspond to unmodelled sensor and actuator dynamics.

3 Passivity analysis of the Orr–Sommerfeld/Squire equations

3.1 Blasius boundary layer

We consider a three-dimensional flow field occupying the region $(x, y, z) \in [0, \infty] \times [a, b] \times [-\infty, \infty]$ with a base parallel laminar flow $(U(y), 0, 0)$ and associated pressure field $P(x, y, z, t)$. The Blasius boundary layer flow (Schlichting, 1979) is depicted in Fig. 3 and we shall take $a = 0$. Although $b \rightarrow \infty$, a finite computational boundary for b will be employed as discussed below. The nominal laminar flow $(U, V, 0)$ is known to be nonparallel ($V \neq 0$), but we shall make the approximation $V = 0$ and take $U(y)$ to be the Blasius solution: $U(y) = df(\eta)/d\eta$ (this has been nondimensionalised using the free-stream velocity U_0) where $\eta = y_d \sqrt{\rho U_0 / (\mu x_d)}$ (x_d, y_d , and z_d refer to dimensional coordinates) and $f(\eta)$ is the solution of $2d^3 f/d\eta^3 + (d^2 f/d\eta^2)f = 0$ with $df(0)/d\eta = f(0) = 0$ and $d^2 f(0)/d\eta^2 = 0.33205733622$ which yields the correct asymptotic boundary condition $df(\eta)/d\eta = 1$ as $\eta \rightarrow \infty$.

The displacement thickness is given by $H = \delta^* = 1.7207876573 \sqrt{\mu x_d / (\rho U_0)}$ where the free-stream velocity is U_0 . The local Reynolds number will be denoted by $Re = \rho U_0 \delta^* / \mu$ where ρ is the fluid density and μ is the absolute viscosity. The displacement thickness δ^* will nondimensionalise length and U_0 will nondimensionalise velocity. As noted above, we will use a finite computational domain with $b = (24/H) \sqrt{\mu x_d / (\rho U_0)}$ (dimensionless) and at this boundary we will impose an inviscid asymptotic solution to be described in the next section.

3.2 Orr–Sommerfeld/Squire equations

Assuming small perturbations $u(x, y, z, t)$, $v(x, y, z, t)$, $w(x, y, z, t)$, and $p(x, y, z, t)$ about the Blasius flow, the linearised incompressible Navier–Stokes equations [10] are

$$\frac{\partial u}{\partial x} + \frac{\partial v}{\partial y} + \frac{\partial w}{\partial z} = 0 \tag{8}$$

$$\frac{\partial u}{\partial t} + U \frac{\partial u}{\partial x} + U'v = -\frac{\partial p}{\partial x} + \frac{1}{Re} \nabla^2 u \tag{9}$$

$$\frac{\partial v}{\partial t} + U \frac{\partial v}{\partial x} = -\frac{\partial p}{\partial y} + \frac{1}{Re} \nabla^2 v \tag{10}$$

$$\frac{\partial w}{\partial t} + U \frac{\partial w}{\partial x} = -\frac{\partial p}{\partial z} + \frac{1}{Re} \nabla^2 w \tag{11}$$

where $U'(y) = dU(y)/dy$ and $\nabla^2 = \partial^2/\partial x^2 + \partial^2/\partial y^2 + \partial^2/\partial z^2$. It has been assumed that quantities are nondimensionalised using the velocity U_0 and distance H . The boundary conditions are taken to be $u(x, a, z, t) = u(x, b, z, t) = v(x, b, z, t) = w(x, a, z, t) = w(x, b, z, t) = 0$ and the control variable is taken to be $v(x, a, z, t)$, which corresponds to wall-normal blowing and suction.

Introducing the wall-normal vorticity

$$\zeta(x, y, z, t) \triangleq \frac{\partial u}{\partial z} - \frac{\partial w}{\partial x} \tag{12}$$

it can be shown [17] that Eqs. (8)–(11) can be simplified to yield equations for the wall-normal velocity v and vorticity ζ :

$$-\nabla^2 \dot{v} + \left\{ U \frac{\partial}{\partial x} \nabla^2 - U'' \frac{\partial}{\partial x} - \nabla^2 \nabla^2 / Re \right\} v = 0 \tag{13}$$

$$\dot{\zeta} + U' \frac{\partial v}{\partial z} + \left\{ U \frac{\partial}{\partial x} - \nabla^2 / Re \right\} \zeta = 0 \tag{14}$$

Introducing the spatial Fourier transform in the x and z directions, or alternatively letting

$$v(x, y, z, t) = \Re \{ \hat{v}(y, t) \exp[i(\alpha x + \beta z)] \} \tag{15}$$

$$\zeta(x, y, z, t) = \Re \{ \hat{\zeta}(y, t) \exp[i(\alpha x + \beta z)] \} \tag{16}$$

where \hat{v} and $\hat{\zeta}$ are the complex amplitudes and α, β are the real wavenumbers, leads to the Orr–Sommerfeld and Squire equations [17]:

$$\begin{bmatrix} \mathcal{M}_{os} & 0 \\ 0 & \mathcal{M}_{sq} \end{bmatrix} \begin{bmatrix} \hat{v} \\ \hat{\zeta} \end{bmatrix} + \begin{bmatrix} \mathcal{K}_{os} & 0 \\ \mathcal{K}_c & \mathcal{K}_{sq} \end{bmatrix} \begin{bmatrix} \hat{v} \\ \hat{\zeta} \end{bmatrix} = \begin{bmatrix} 0 \\ 0 \end{bmatrix} \tag{17}$$

where

$$\mathcal{M}_{os} = -\Delta, \quad \mathcal{M}_{sq} = \mathcal{I}, \quad \Delta = \partial^2/\partial y^2 - \alpha^2 - \beta^2 \tag{18}$$

$$\mathcal{K}_{os} = -i\alpha U \Delta + i\alpha U'' + \Delta \Delta / Re, \quad \mathcal{K}_c = i\beta U', \tag{19}$$

$$\mathcal{K}_{sq} = i\alpha U - \Delta / Re \tag{20}$$

and \mathcal{I} is the identity operator. The boundary conditions are $\hat{v}_y(a, t) = \hat{\zeta}(a, t) = 0$, $\hat{v}(b, t) = -k\hat{v}_y(b, t)$ (the inviscid asymptotic) and $\hat{\zeta}(b, t) = 0$. The (real) control inputs are taken to be

$$\mathbf{v}(t) = [\Re\{\hat{v}(a, t)\} \Im\{\hat{v}(a, t)\}]^T = [v_r(t) \ v_i(t)]^T \tag{21}$$

(the vector \mathbf{v} should not be confused with the scalar velocity components u and v ; note that the symbol v will not be used in this paper to refer to a fluid's kinematic viscosity).

3.3 Passivity analysis

In this section, it will be assumed that $b \rightarrow \infty$ with boundary conditions $\hat{v}_y(a, t) = \hat{v}_y(b, t) = \hat{v}(b, t) = 0$, and $\hat{\zeta}(a, t) = \hat{\zeta}(b, t) = 0$. The energy $E(t) \geq 0$ is taken to be [17]

$$\begin{aligned} E(t) &= \frac{\alpha\beta}{8\pi^2} \int_0^{2\pi/\beta} \int_0^{2\pi/\alpha} \int_a^b (u^2 + v^2 + w^2) dy dx dz \\ &= E_{os}(t) + E_{sq}(t) \end{aligned}$$

where

$$E_{os} = \frac{1}{4k^2} \int_a^b (\hat{v}_y^* \hat{v}_y + k^2 \hat{v}^* \hat{v}) dy, \quad E_{sq} = \frac{1}{4k^2} \int_a^b \hat{\zeta}^* \hat{\zeta} dy \geq 0$$

and $k^2 = \alpha^2 + \beta^2$. (Note that the subscript notation $()_y$ indicates the corresponding partial derivative; the superscript $()^*$ denotes the complex conjugate). Taking the time derivative of these two equations yields

$$2k^2 \dot{E}_{os} = \frac{1}{2} \int_a^b (\hat{v}_y^* \dot{\hat{v}}_y + \dot{\hat{v}}_y^* \hat{v}_y + k^2 \dot{\hat{v}}^* \hat{v} + k^2 \hat{v}^* \dot{\hat{v}}) dy$$

$$2k^2 \dot{E}_{sq} = \frac{1}{2} \int_a^b (\dot{\hat{\zeta}}^* \hat{\zeta} + \hat{\zeta}^* \dot{\hat{\zeta}}) dy$$

Integrating the first two terms by parts and introducing the boundary conditions, the Orr–Sommerfeld equation, the Squire equation, and their complex conjugates leads to equations in which the terms containing D^4 can be integrated by parts twice and the terms containing D^2 once, while enforcing the boundary conditions, to arrive at

$$\begin{aligned} 2k^2 \dot{E}_{os} &= -Re^{-1} \left(\int_a^b k^4 |\hat{v}|^2 + 2k^2 |D\hat{v}|^2 + |D^2\hat{v}|^2 \right) dy \\ &\quad - \alpha \int_a^b U'(y) \Im\{\hat{v}\hat{v}_y^*\} dy + Re^{-1} \Re\{\hat{v}^* D^3 \hat{v}\}_{y=a} \end{aligned} \tag{22}$$

$$2k^2 \dot{E}_{sq} = -Re^{-1} \left(|D\hat{\zeta}|^2 + k^2 |\hat{\zeta}|^2 \right) dy - \beta \int_a^b U'(y) \Im\{\hat{v}^* \hat{\zeta}\} dy \tag{23}$$

Since $\hat{u} = (i/k^2)(\alpha D\hat{v} - \beta\hat{\zeta})$, the sum of these equations can be simplified to

$$2k^2\dot{E} = -Re^{-1} \left(\int_a^b k^4|\hat{v}|^2 + 2k^2|D\hat{v}|^2 + |D^2\hat{v}|^2 + |D\hat{\zeta}|^2 + k^2|\hat{\zeta}|^2 \right) dy - k^2 \int_a^b U'(y)\Re e[\hat{u}^*\hat{v}] dy + Re^{-1}\Re e[\hat{v}^*D^3\hat{v}]_{y=a} \quad (24)$$

In the hopes of obtaining a passive input–output pair, the observation is defined to be

$$\mathbf{m}_{os}(t) = [\Re e\{D^3\hat{v}(a, t)\} \Im m\{D^3\hat{v}(a, t)\}]^T = [m_{os,r}(t) \ m_{os,i}(t)]^T. \quad (25)$$

In the next section, it will be demonstrated that the output \mathbf{m}_{os} can be obtained from physically measurable pressure quantities at the wall.

Now, noting that $\Re e[\hat{v}^*D^3\hat{v}]_{y=a} = \mathbf{m}_{os}^T(t)\mathbf{v}(t)$, while integrating Eq. (22) with respect to time, yields

$$\int_0^T \mathbf{m}_{os}^T \mathbf{v} dt = \int_0^T \int_a^b \left(k^4|\hat{v}|^2 + 2k^2|D\hat{v}|^2 + |D^2\hat{v}|^2 \right) dy dt + 2k^2 Re E_{os}(T) + \alpha Re \int_0^T \int_a^b U'(y)\Re e[\hat{v}_y^*\hat{v}] dy dt - 2k^2 Re E_{os}(0) \quad (26)$$

Clearly, the first three integrated terms on the right-hand side of these two equations, as well as $2k^2 Re E_{os}(T)$, are non-negative. However, the term containing $U'(y)$ is indefinite and, potentially, destroys the passivity of the mapping from the input \mathbf{v} to the output \mathbf{m}_{os} . In the absence of this term, the mapping is passive. In particular, for $\alpha = 0$, we have from Eq. (26), that

$$\int_0^T \mathbf{m}_{os}^T \mathbf{v} \Big|_{\alpha=0} dt \geq \delta = -2\beta^2 Re E_{os}(0) \quad (27)$$

which is a statement of passivity. This can be significant because it was shown by Butler and Farrell [7] that for $Re = 1000$, the case of maximum transient growth occurs for $\alpha = 0$, $\beta = 0.65$. In physical terms, Eq. (27) states that the work done on the fluid as measured by the sensor/actuator combination is non-negative (neglecting the initial conditions); hence, the work done by the fluid is not positive indicating that it only stores or consumes energy.

In general, there are stabilising influences to be had using this sensor/actuator pair. For example, using the simplest strictly passive output feedback law, $\mathbf{v}(t) = -\bar{K}\mathbf{m}_{os}(t)$, $\bar{K} > 0$, may lead to a stable closed-loop sys-

tem. Introducing it into Eq. (24) yields

$$\dot{E} = -(2k^2 Re)^{-1} \left(\int_a^b k^4|\hat{v}|^2 + 2k^2|D\hat{v}|^2 + |D^2\hat{v}|^2 + |D\hat{\zeta}|^2 + k^2|\hat{\zeta}|^2 \right) dy - (2k^2 Re)^{-1} \bar{K} \mathbf{m}_{os}^T \mathbf{m}_{os} - \frac{1}{2} \int_a^b U'(y)\Re e[\hat{u}^*\hat{v}] dy \quad (28)$$

which demonstrates the potential of the output feedback law to lead to an energy-dissipative closed-loop system if the two terms containing $(2k^2 Re)^{-1}$ are able to dominate the last term. Similar results can be obtained using an SPR controller which essentially mimics a positive definite gain on a frequency-by-frequency basis.

3.4 Measurements

Taking the Fourier transform of the continuity equation in Eq. (8) while differentiating twice with respect to y yields

$$\hat{v}_{yyy} = -i(\alpha\hat{u}_{yy} + \beta\hat{w}_{yy}) \quad (29)$$

Taking the Fourier transform of Eqs. (9) and (10) and evaluating at the lower wall [with $\hat{u}(a, t) = \hat{w}(a, t) = 0$] yields

$$U'(a)\hat{v}(a, t) = -i\alpha\hat{p}(a, t) + \frac{1}{Re}\hat{u}_{yy}(a, t) \\ 0 = -i\beta\hat{p}(a, t) + \frac{1}{Re}\hat{w}_{yy}(a, t)$$

Multiplying the first of these by α and the second by β and adding the results produces $\alpha\hat{u}_{yy} + \beta w_{yy} = Re[\alpha U'(a)\hat{v}(a, t) + ik^2\hat{p}]$. When this is substituted into Eq. (29), we arrive at

$$\hat{v}_{yyy}(a, t) = Re k^2 \hat{p}(a, t) - i Re \alpha U'(a) \hat{v}(a, t) \quad (30)$$

which is the desired result. This shows that the special output identified above, \mathbf{m}_{os} , is obtainable from pressure measurements at the wall and knowledge of the control input \mathbf{v} . In the case where $\alpha = 0$, the control input is not required.

3.5 Nonlinear passivity analysis

In this section, we will find it helpful to define wall functions using the notational paradigm

$$v_w(x, z, t) = v(x, a, y, t) \quad (31)$$

with corresponding two-dimensional spatial Fourier transform

$$\hat{v}_{w,\alpha\beta}(t) = \int_{-\infty}^{\infty} \int_0^{\infty} v_w(x, z, t) \exp[-i(\alpha x + \beta z)] dx dz \tag{32}$$

(note that the wave number dependence has been explicitly indicated.) It will be helpful to introduce an inner product for wall functions:

$$\begin{aligned} \langle \mathbf{m}_w, \mathbf{e}_w \rangle_{T,w} &= \int_0^T \int_{-\infty}^{\infty} \int_0^{\infty} \mathbf{m}_w^T \mathbf{e}_w dx dz dt \\ &= \frac{1}{4\pi^2} \int_0^T \int_{-\infty}^{\infty} \int_{-\infty}^{\infty} \Re\{ \hat{\mathbf{m}}_w^H \hat{\mathbf{e}}_w \} d\alpha d\beta dt \end{aligned} \tag{33}$$

where we have used Parseval's theorem for the latter expression.

We introduce an extended space of wall functions according to $L_{2e,w} = \{ \mathbf{e}_w \mid \langle \mathbf{e}_w, \mathbf{e}_w \rangle_{T,w} < \infty, 0 \leq T < \infty \}$. Consider a system $\mathcal{H}_w : L_{2e,w} \rightarrow L_{2e,w}$ with input \mathbf{e}_w and output $\mathbf{m}_w = \mathcal{H}_w \mathbf{e}_w$. We will say that \mathcal{H}_w is in the conic sector $[a_c, b_c]$ where $a_c < b_c$ with $b_c > 0$ if

$$\begin{aligned} -\frac{1}{b_c} \langle \mathcal{H}_w \mathbf{e}_w, \mathcal{H}_w \mathbf{e}_w \rangle_{T,w} + \left(1 + \frac{a_c}{b_c} \right) \langle \mathbf{e}_w, \mathcal{H}_w \mathbf{e}_w \rangle_{T,w} \\ - a_c \langle \mathbf{e}_w, \mathbf{e}_w \rangle_{T,w} \geq 0 \end{aligned} \tag{34}$$

$\forall \mathbf{e}_w \in L_{2e,w}, T \geq 0$. Comparing this with Eq. (3), it is clear that the inner product and corresponding norm have been generalized from temporal functions to functions of both space and time on the wall.

Using the Parseval relation on this, we can write the conic sector relation as

$$\begin{aligned} \frac{1}{4\pi^2} \int_{-\infty}^{\infty} \int_{-\infty}^{\infty} \int_0^T \left[-\frac{1}{b_c} \hat{\mathbf{m}}_{w,\alpha\beta}^H \hat{\mathbf{m}}_{w,\alpha\beta} \right. \\ \left. + \left(1 + \frac{a_c}{b_c} \right) \Re\{ \hat{\mathbf{m}}_{w,\alpha\beta}^H \hat{\mathbf{e}}_{w,\alpha\beta} \} - a_c \hat{\mathbf{e}}_{w,\alpha\beta}^H \hat{\mathbf{e}}_{w,\alpha\beta} \right] \\ dt d\alpha d\beta \geq 0 \end{aligned} \tag{35}$$

Making the identifications $\hat{\mathbf{e}}_w = \hat{v}_w$, $\hat{\mathbf{m}}_w = \hat{v}_{yyy,w}$, and recalling the definitions in Eqs. (21) and (25), the above can be written as:

$$\begin{aligned} \frac{1}{4\pi^2} \int_{-\infty}^{\infty} \int_{-\infty}^{\infty} \int_0^T \left[-\frac{1}{b_c} \mathbf{m}_{os,\alpha\beta}^T \mathbf{m}_{os,\alpha\beta} \right. \\ \left. + \left(1 + \frac{a_c}{b_c} \right) \mathbf{m}_{os,\alpha\beta}^T \mathbf{v}_{\alpha\beta} - a_c \mathbf{v}_{\alpha\beta}^T \mathbf{v}_{\alpha\beta} \right] \\ dt d\alpha d\beta \geq 0 \end{aligned} \tag{36}$$

where we have explicitly indicated the spatial wavenumber dependence on (α, β) . Hence, if the mapping from $\mathbf{v}_{\alpha\beta}(t)$ to $\mathbf{m}_{os,\alpha\beta}(t)$ is in the conic sector $[a_c, b_c]$ for each wavenumber pair (α, β) (that is the inner integral with respect to time is non-negative for each wavenumber pair (α, β)), then the corresponding wall operator \mathcal{H}_w is in the conic sector $[a_c, b_c]$ (that is the triple integral with respect to space and time is non-negative). This justifies an approach to controller design which seeks to stabilise the system with individual controller designs at each wavenumber pair (α, β) .

Hence, if the mapping from $\mathbf{v}_{\alpha\beta}(t)$ to $\mathbf{m}_{os,\alpha\beta}(t)$ is expressed in the (temporal) frequency domain as $\mathbf{m}_{os,\alpha\beta}(s) = \mathbf{G}_{\alpha\beta}(s) \mathbf{v}_{\alpha\beta}(s)$ then one can seek a feedback controller design at each (α, β) pair according to $\mathbf{v}_{\alpha\beta}(s) = -\mathbf{K}_{\alpha\beta}(s) \mathbf{m}_{os,\alpha\beta}(s)$ with corresponding closed-loop transfer matrix $\mathbf{H}_{\alpha\beta}(s) = \mathbf{G}_{\alpha\beta}(s) [\mathbf{I} + \mathbf{K}_{\alpha\beta}(s) \mathbf{G}_{\alpha\beta}(s)]^{-1}$. If $\mathbf{K}_{\alpha\beta}(s)$ can be designed such that $\mathbf{H}_{\alpha\beta}(s)$ satisfies Eq. (4) at each value of (α, β) , then the corresponding operator \mathcal{H}_w in the combined time and space domains will also be in the cone $[a_c, \infty]$. This approach to controller design is depicted in Fig. 4. In this figure, the blocks FT and IFT correspond to the (spatial) Fourier transform and its inverse, respectively. The block \mathcal{N} corresponds to a parallel feedforward representing the nonlinear part of the mapping from v_w to $v_{yyy,w}$.

Let us express the time and space domain mapping from v_w to $v_{yyy,w}$ as

$$v_{yyy,w} = \mathcal{L}(v_w) + \mathcal{N}(v_w) \tag{37}$$

where \mathcal{L} is the linear mapping expressed in Eq. (30) and \mathcal{N} is nonlinear. Consider the fully nonlinear incompressible Navier–Stokes equations describing the flow field $(U(y) + u, v, w)$ and the pressure field $P + p(x, y, z, t)$ (the precursor of the linearised equations in Eqs. (8)-(11); we do not write them down to conserve space). If one differentiates the nonlinear version of Eq. (9) with respect to x , the nonlinear version of Eq. (10) with respect to y , and the nonlinear version of Eq. (11) with respect to z and evaluates them at the wall, one arrives at

$$p_{xx,w} = \frac{1}{Re} \nabla^2 u_{x,w} - U'(a) v_{x,w} \tag{38}$$

$$p_{yy,w} = \frac{1}{Re} \nabla^2 v_{y,w} - U'(a) v_{x,w} \tag{39}$$

$$p_{zz,w} = \frac{1}{Re} \nabla^2 w_{z,w} \tag{40}$$

where the no-slip boundary conditions have been applied in conjunction with the continuity equation. Interestingly, one arrives at the same equations using the linearised Navier–Stokes equations.

Using Eq. (39), one can write

$$v_{yyy,w} = \mathcal{L}(v_w) + \mathcal{N}(v_w) = Re(p_{yy,w} + U'(a)v_{x,w}) \tag{41}$$

v_1 to the right-hand side of the equation to form the control input. We also set $v'_{N_e+1} = -kv_{N_e+1}$. Defining $\mathbf{q}_{os} = [v_2 \ v'_2 \ \dots \ v_{N_e} \ v'_{N_e} \ v_{N_e+1}]^T$, $\mathbf{q}_{sq} = [\zeta'_1 \ \zeta_2 \ \zeta'_2 \ \dots \ \zeta_{N_e} \ \zeta'_{N_e} \ \zeta'_{N_e+1}]^T$, $\mathbf{q} = [\mathbf{q}_{os}^T \ \mathbf{q}_{sq}^T]^T$, and removing the appropriate rows and columns from the above equation yields

$$\mathbf{M}_r \dot{\mathbf{q}} + (\mathbf{K}_r + i\mathbf{K}_i)\mathbf{q} = (\mathbf{B}_{1r} + i\mathbf{B}_{1i})v_1 + \mathbf{B}_{2r}\dot{v}_1 \quad (49)$$

where \mathbf{M}_r , \mathbf{K}_r , and \mathbf{K}_i are the reduced matrices which can be partitioned analogous to those in Eq. (48). Additional terms are added to the last row and last column of each Orr–Sommerfeld matrix on the left-hand side to enforce $v'_{N_e+1} = -kv_{N_e+1}$. It is straightforward to form \mathbf{B}_{1r} from the entries of $\widehat{\mathbf{K}}_{os,r}$, \mathbf{B}_{1i} from the entries of $\widehat{\mathbf{K}}_{os,i}$ and $\widehat{\mathbf{K}}_{c,i}$, and \mathbf{B}_{2r} from the entries of $\widehat{\mathbf{M}}_{os,r}$.

Now, take the (real) control input to be $\mathbf{e} = [\Re\{v_1\} \ \Im\{v_1\}]^T$ and the (real) measurement output is taken to be $\mathbf{m}(t) = \mathbf{m}_{os}(t) = [\Re\{\hat{v}_{yyy}(a, t)\} \ \Im\{\hat{v}_{yyy}(a, t)\}]^T$. If the (real) state vector is taken as $\mathbf{x} = [\mathbf{q}_{os,r}^T \ \mathbf{q}_{os,i}^T \ \mathbf{q}_{sq,r}^T \ \mathbf{q}_{sq,i}^T]^T - \text{blockdiag}\{\mathbf{M}_r^{-1}\mathbf{B}_{2r}, \mathbf{M}_r^{-1}\mathbf{B}_{2r}\}\mathbf{e}$ where $\mathbf{q}_{os,r} = \Re\{\mathbf{q}_{os}\}$, $\mathbf{q}_{os,i} = \Im\{\mathbf{q}_{os}\}$, $\mathbf{q}_{sq,r} = \Re\{\mathbf{q}_{sq}\}$, $\mathbf{q}_{sq,i} = \Im\{\mathbf{q}_{sq}\}$, then the methods of Damaren [8] can be used to derive a state-space model of the form in Eqs. (1) and (2).

If \mathbf{x} is partitioned as $\mathbf{x} = \text{col}\{\mathbf{x}_{os}, \mathbf{x}_{sq}\}$, then the matrices in the state-space model can be partitioned as

$$\mathbf{A} = \begin{bmatrix} \mathbf{A}_{os} & \mathbf{0} \\ \mathbf{A}_c & \mathbf{A}_{sq} \end{bmatrix}, \mathbf{B} = \begin{bmatrix} \mathbf{B}_{os} \\ \mathbf{B}_{sq} \end{bmatrix}, \mathbf{C} = [\mathbf{C}_{os} \ \mathbf{C}_{sq}], \mathbf{D} \quad (50)$$

Given the structure of \mathbf{A} , the modes can be decomposed into two sets [17]. The Orr–Sommerfeld modes correspond to the eigenvalues of \mathbf{A}_{os} with eigenvectors of the form $\bar{\mathbf{x}} = \text{col}\{\bar{\mathbf{x}}_{os}, \bar{\mathbf{x}}_{sq}\}$ (note that $\bar{\mathbf{x}}_{sq} = \mathbf{0}$ when $\beta = 0$ since $\mathbf{A}_c = \mathbf{0}$ in that case). The Squire modes correspond to eigenvalues of \mathbf{A}_{sq} with eigenvectors of the form $\bar{\mathbf{x}} = \text{col}\{\mathbf{0}, \bar{\mathbf{x}}_{sq}\}$. Hence, there is the possibility that both the Orr–Sommerfeld and Squire modes are controllable using \mathbf{e} . However, all of the Squire modes are completely unobservable using the output \mathbf{m}_{os} for which $\mathbf{C}_{sq} = \mathbf{0}$. This can be mitigated to some extent because all of the Squire modes are asymptotically stable [17] and hence are stabilisable. However, it was noted by Butler and Farrell [7] that the initial conditions contributing the most to transient energy growth contained streamwise vortices. Given that the stability properties predicted by the passivity theorem are input–output results, we do not speculate on the ability of the proposed input/output combination to suppress large transient growth imparted by the initial conditions.

Table 1 Orr–Sommerfeld/Squire eigenvalues for Blasius case, $Re = 800$, $\alpha = 0.25$, $\beta = 0.2$

Schmid and Henningson		Damaren ($N_e = 240$, $b = 24$)	
$\Re\{\lambda/\alpha\}$	$\Im\{\lambda/\alpha\}$	$\Re\{\lambda/\alpha\}$	$\Im\{\lambda/\alpha\}$
Orr–Sommerfeld			
+ 0.00287572	0.39065421	+ 0.002826	0.390610
– 0.23434181	0.54772364	– 0.234257	0.547720
– 0.31005379	0.33866341	– 0.309990	0.338641
– 0.37872068	0.79181869	– 0.378502	0.791717
– 0.40505900	0.65749147	– 0.404910	0.657402
Squire			
– 0.13769021	0.23869653	– 0.137679	0.238688
– 0.23747142	0.41904327	– 0.237431	0.419016
– 0.31360121	0.57017612	– 0.313527	0.570123
– 0.37342899	0.70889059	– 0.373318	0.708801
– 0.41937502	0.84255313	– 0.419228	0.842414

5 Numerical example

In an effort to validate our numerical approach, we begin by considering $N_e = 240$ finite elements and an upper edge dimension of $b = 24$. Given the availability of data from Schmid and Henningson, [17], the initial parameters are taken to be $Re = 800$, $\alpha = 0.25$, $\beta = 0.2$. The ensuing discrete spectrum that is obtained from the eigenvalues of \mathbf{A} in Eq. (50) is given in Table 1 along with the corresponding values from Schmid and Henningson [17]. In general, there is agreement to four significant figures with the exception of the unstable mode at $+0.0029 \pm i0.3907$ which only agrees with two significant figures.

For the case $Re = 800$, $\alpha = 0$, $\beta = 0.2$, the corresponding multivariable Nyquist plot of $\mathbf{G}(s) = \mathbf{C}(s\mathbf{I} - \mathbf{A})^{-1}\mathbf{C} + \mathbf{D}$ (i.e., the eigenloci of $\mathbf{G}(i\omega)$) is given in Fig. 5 for $\mathbf{m} = \mathbf{m}_{os}$. The eigenvalues λ_j have been scaled to $(4/\pi) \tan^{-1}(|\lambda_j|)[\exp(i \arg(\lambda_j))]$ which preserves the phase, maps zero to zero, maps the unit circle onto the unit circle, and maps ∞ onto a circle with radius two. Clearly, this transfer matrix is positive real (since $\Re\{\lambda_j[\mathbf{G}(i\omega)]\} \geq 0$) as predicted by our passivity analysis in Sect. 3. It is straightforward to verify that a non-negative Hermitian part of $\mathbf{G}(i\omega)$ corresponds to $\Re\{\lambda_j[\mathbf{G}(i\omega)]\} \geq 0$.

Let us return to the case $Re = 800$, $\alpha = 0.25$, and $\beta = 0.20$ which is unstable (and hence nonpassive). Examining the eigenvalues of $\mathbf{A} - \mathbf{B}\mathbf{D}^{-1}\mathbf{C}$ reveals a zero at $s = 0.2412$ and hence the system is unstable and nonminimum phase. However, as intimated in Eq. (28) et seq., energy dissipativeness may be possible using an SPR controller. To illustrate this, we employed the design procedure of Sec. 2.2 using a reduced-order modal model with the 16 most controllable/observable modes and $\mathbf{Q} = \mathbf{C}_r^T \mathbf{C}_r$ (it is only positive

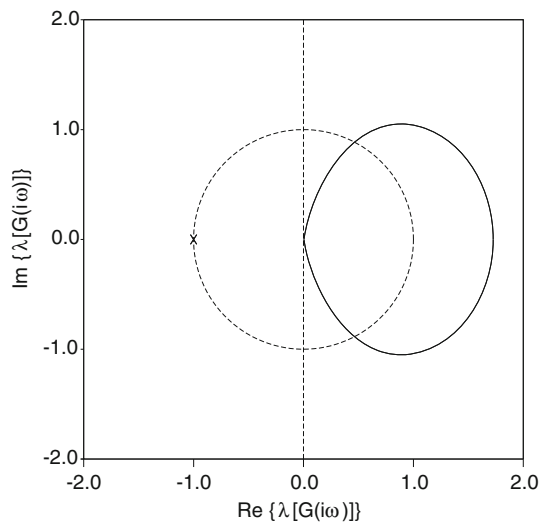


Fig. 5 Nyquist plot ($m = m_{os}$, $Re = 800$, $\alpha = 0$, $\beta = 0.2$)

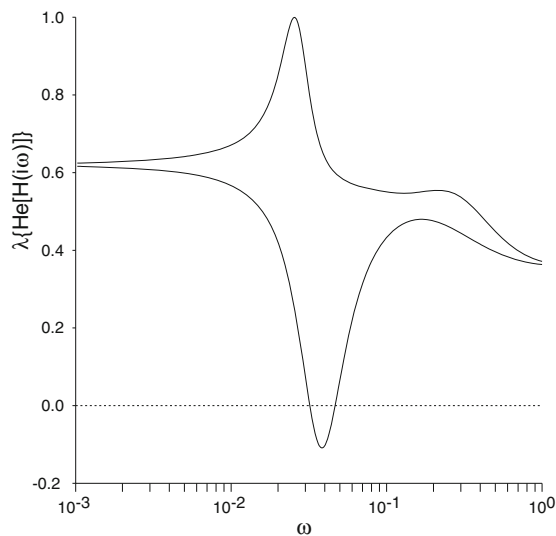


Fig. 6 Eigenvalues of the Hermitian part of the closed-loop transfer matrix $H(s)$ using reduced-order SPR control

semidefinite in this case), $R = I$, and $Q_c = 5I$, where C_r is the output matrix of the reduced-order model. This leads to a stable closed-loop system. The eigenvalues of the Hermitian part of the closed-loop transfer matrix from d_1 to $m_1 = m_{os}$ ($H(s) = G(s)[I + K(s)G(s)]^{-1}$) are depicted in Fig. 6. Although $K(s)$ is determined using a reduced-order model, the closed-loop stability calculation and the determination of $H(s)$ make use of the full-order model of $G(s)$. Given the negative excursion of the smallest eigenvalue, we conclude that $H(s)$ is not positive real since $a_c \doteq -0.108$. However, it does belong to the conic sector $[a_c, \infty]$ and hence is guaranteed to be stable when placed in negative feedback with an uncertainty block Δ strictly belonging to the conic sector $(0, -1/a_c)$.

6 Conclusions

The important property of passivity has been examined in the case of the boundary-feedback controlled Orr–Sommerfeld/Squire equations. A study of the work-energy balance was used to select the appropriate sensed variables corresponding to wall-normal velocity actuation. This corresponded to the third derivative (wall-normal direction) of the wall-normal velocity, which it was demonstrated can be constructed from pressure measurements made along the wall. This choice of sensing and actuation was shown to lead to passivity when the streamwise wavenumber α was equal to zero. This was validated by looking at the Nyquist plot for a typical case. Unfortunately, the Squire modes are not observable from this output which limited its applicability. However, it was shown that stabilisation could be achieved in an unstable case using a strictly positive real controller and this output. An analysis was presented that showed that a series of stabilising linear designs at each wavenumber pair could provide stability of the original nonlinear distributed parameter system.

Compliance with ethical standards

Conflict of interest The author declares that he has no conflict of interest.

References

1. Bagheri S, Brandt L, Henningson DS (2009) Input-output analysis, model reduction, and control of the flat-plate boundary layer. *J Fluid Mech* 620:263–298
2. Belson BA, Semeraro O, Rowley CW, Henningson DS (2013) Feedback control of instabilities in the two-dimensional blasius boundary layer: the role of sensors and actuators. *Phys Fluids* 25:054106
3. Benhabib RJ, Iwens RP, Jackson RL (1981) Stability of large space structure control systems using positivity concepts. *J Guidance Control* 4:487–494
4. Bewley TR (2001) Flow control: new challenges for a new renaissance. *Prog Aerosp Sci* 37:21–58
5. Bewley TR, Liu S (1998) Optimal and robust control and estimation of linear paths to transition. *J Fluid Mech* 365:305–349
6. Bridgeman LJ, Forbes JR (2014) Conic-sector-based control to circumvent passivity violations. *Int J Control* 87(8):1467–1477
7. Butler KM, Farrell BF (1992) Three-dimensional optimal perturbations in viscous shear flow. *Phys Fluids A: Fluid Dyn* 4(8):1637–1650
8. Damaren CJ (2016) Laminar-turbulent transition control using passivity analysis of the Orr–Sommerfeld equation. *J Guidance Control Dyn* 39(7):1602–1613
9. Desoer CA, Vidyasagar M (1975) Feedback systems: input-output properties. Academic Press, Cambridge
10. Drazin PG, Reid WH (1981) Hydrodynamic stability. Cambridge University Press, Cambridge
11. Heins PH, Jones BL, Sharma AS (2016) Passivity-based output-feedback control of turbulent channel flow. *Automatica* 69:348–355

12. Joshi SS, Speyer JL, Kim J (1997) A systems theory approach to the feedback stabilization of infinitesimal and finite-amplitude disturbances in plane poiseuille flow. *J Fluid Mech* 332:157–184
13. Kim J, Bewley TR (2007) A linear systems approach to flow control. *Ann Rev Fluid Mech* 39:383–417
14. Mamou M, Khalid M (2004) Finite element solution of the Orr–Sommerfeld equation using high precision hermite elements: plane poiseuille flow. *Int J Numer Methods Fluids* 44:721–735
15. Safonov MG, Jonckheere EA, Verma M, Limebeer DJN (1987) Synthesis of positive real multivariable feedback systems. *Int J Control* 45(3):817–842
16. Schlichting H (1979) *Boundary-layer theory*, 7th edn. McGraw-Hill, New York
17. Schmid PJ (2001) *Stability and transition in shear flows*. Springer, New York
18. Sharma AS, Morrison JF, McKeon BJ, Limebeer DJN, Koberg WH, Kerwin SJ (2011) Relaminarisation of $Re_T = 100$ globally stabilising linear feedback control. *Phys Fluids* 23:125105
19. Vidyasagar M (1992) *Nonlinear control systems*, 2nd edn. Prentice-Hall Inc, Upper Saddle River
20. Zames G (1966) On the input-output stability of time-varying nonlinear feedback systems. Part I: conditions derived using concepts of loop gain, conicity, and positivity. *IEEE Trans Autom Control* 11(2):228–238